

Article

Forest Plant Water Utilization and the Eco-Hydrological Regulation in the Karst Desertification Control Drainage Area

Bo Fan ^{1,2}, Kangning Xiong ^{1,2,*}  and Ziqi Liu ^{1,2}

¹ School of Karst Science, Guizhou Normal University, Guiyang 550001, China; 17793689707@163.com (B.F.); 201511004@gznu.edu.cn (Z.L.)

² State Engineering Technology Institute for Karst Desertification Control, Guiyang 550001, China

* Correspondence: xiongkn@163.com

Abstract: Subtropical forests in southwestern karst areas are the top priority for ecosystem restoration, as studying the water absorption strategies of the major plants in these regions is crucial to determining the species distribution and coexistences within these seasonal subtropical forests, which will help us to cope with the forest ecosystem crisis under future climate change. We used the stable isotope ratios (δD and $\delta^{18}O$) of tree xylem and soil water to assess the seasonal changes in the water use patterns and hydrological niche separations of four dominant tree species in seasonal subtropical forests in southwestern karst areas. The results showed that the soil water's isotopic composition varied gradiently in the vertical direction and that the variation of the soil water's isotopic composition was greater in the shallow layer than in its depths. *Juglans regia* (HT) mainly depended on soil water at a depth of 30–60 cm ($41.8 \pm 6.86\%$) and fissure water ($32.5 \pm 4.21\%$), while *Zanthoxylum bungeanum* Maxim (HJ) and *Eriobotrya japonica* Lindl (PP) had the same water use pattern. In the dry season, HT competed with HJ and PP for water resources, and in the rainy season, HJ and PP competed with *Lonicera japonica* (JYH), while HJ competed with PP all the time. JYH and HT were in a separate state of hydrologic niche and they did not pose a threat to each other. Coexisting trees are largely separated along a single hydrological niche axis that is defined by their differences in root depth, which are closely related to tree size. Our results support the theory of hydrological niche isolation and its potential responses in relation to drought resistance. This study provides a method for determining more efficient plant combinations within karst forest vegetation habitats and its results will have important implications for ecosystem vegetation restoration.

Keywords: karst forest; vegetation water use strategy; hydrogen and oxygen stable isotopes; hydrologic niche separation



Citation: Fan, B.; Xiong, K.; Liu, Z. Forest Plant Water Utilization and the Eco-Hydrological Regulation in the Karst Desertification Control Drainage Area. *Forests* **2023**, *14*, 747. <https://doi.org/10.3390/f14040747>

Academic Editor: Roberto Tognetti

Received: 17 February 2023

Revised: 29 March 2023

Accepted: 4 April 2023

Published: 5 April 2023



Copyright: © 2023 by the authors. Licensee MDPI, Basel, Switzerland. This article is an open access article distributed under the terms and conditions of the Creative Commons Attribution (CC BY) license (<https://creativecommons.org/licenses/by/4.0/>).

1. Introduction

According to the Global Forest Resources Assessment 2020, the average global forest coverage rate is 31.7% [1], and these forests play an irreplaceable role in maintaining the Earth's ecological and hydrological cycles. Forest distribution and abundance are mainly restricted by water resources [2,3]. Over the last few decades, due to major changes in the climate because of human influence, droughts have become more severe and frequent [4], which will have an obvious influence on the survival of forest vegetation species and the hydrological cycle [5]. Therefore, studying the water use of forest vegetation is crucial for forest ecohydrological regulation [6]. Forest vegetation is a participant in various important processes of the terrestrial hydrological cycle, and its ecological processes and hydrological processes are intertwined. The forest water cycle is an important part of the land water cycle [7,8], as it not only affects the structure, function, and distribution pattern of forest vegetation, but also affects the energy budget, conversion, and distribution of the Earth's surface system. It plays an important role in the carbon and nitrogen balance of terrestrial ecosystems [9–11]. The hydrological function of the forest ecosystem is not only

an important part of its service function, but also affects the system's productivity, nutrient cycle, and other functions [12–14]. Water is a key factor affecting the material circulation and plant growth in forest ecosystems [15]. Plants absorb water from the soil through their roots and store it in their xylem, and they use this water in photosynthesis or lose the water through evaporation via their stomata to complete the hydrological cycle [16].

Affected by the subtropical climate, subtropical forests are mainly found in karst areas in southwest China [17], where water and energy are abundant in the region. However, seasonal droughts always occur due to the inconsistent distribution of temperature and precipitation during the summer [18,19]. In the current extreme arid climate, more and more species are suffering from water stress [20]. The main problem of karst forest ecosystem restoration is vegetation restoration [21]. Understanding the physiological characteristics, ecological characteristics, and water use patterns of the different vegetation in these regions is a necessary means for this vegetation restoration. Stable hydrogen ($\delta^2\text{H}$) and oxygen ($\delta^{18}\text{O}$) isotopes are the most effective tools for determining plant water sources. Previous studies have shown that the isotopic fractionation of water does not occur during root absorption and transport. Thus, the relative contributions of different water sources can be inferred by comparing the $\delta^2\text{H}$ and $\delta^{18}\text{O}$ values of xylowater with the potential water sources (e.g., soil water, groundwater, and rainwater) [22]. Previous studies on subtropical forests have shown that multiple species living in the same habitat may have different water use patterns; this makes it possible for these species to coexist [23], which is called hydroecological niche separation [24]. Symbiotic plants often adopt different water use patterns due to differences in their root size, root depth, and leaf water use, resulting in the spatial–temporal distribution of their water use [25]. Some studies have shown that grasses and herbs tend to draw water from shallow soils throughout the growing season [26,27]. In contrast, some trees and shrubs often have the ability to obtain water from deep soil [22]. In addition, some species have the ability to switch between these shallow and deep soil layers to absorb their water, which is related to the plant's root morphology, as two forms of roots provide them with the ability to use water flexibly, have a high ecological plasticity, and can greatly adapt to changes in the external environment [17,28]. Based on this, plant species with hydrologic niche separation can have symbiosis within the same lifetime without water competition, which is an important mechanism for influencing the plant community structure and maintaining the plant coexistence in ecosystems with limited water resources.

The Guizhou Province is the most threatened area of rocky desertification in southwest China, so the growth and development of its forest plants have received strong attention. The region is widely mountainous, with a high bare rock leakage rate and shallow and discontinuous soil layers [21]. An inappropriate species selection for its forest ecosystem restoration would result in soil dryness vegetation degradation and reforestation difficulties. We know very little about the water uptake of its local species and whether the mix of these species within the small habitats of its subtropical forests is reasonable; therefore, it is urgent to understand the water use strategies of its forest vegetation and whether there is water competition or hydrologic niche separation among its different species.

In this study, stable hydrogen ($\delta^2\text{H}$) and oxygen ($\delta^{18}\text{O}$) isotopes were used to analyze the water use patterns of forest plants in a karst rocky desertification area. Our objectives were to: (1) explore the water use strategies and seasonal variations of the functional vegetation within the forest, and (2) determine whether there was hydroecological niche separation among the forest's species within the same lifetime. We hypothesized that: (i) the water use patterns of the four plants were different, and (ii) there was a significant hydrologic niche separation among the plants within the study habitat. The results of this study will elucidate the characteristics of the water use patterns of plants in karst forests and provide a scientific basis for the coexistence of plants in native territories.

2. Materials and Methods

2.1. Study Area

This study was conducted in the Guizhou Plateau canyon landform-type area in southwest China, which represents the general structure of the karst environmental types in southern China, specifically in the Huajiang section of the Beipanjiang Gorge, Guizhou Province ($105^{\circ}36'30''\sim 105^{\circ}46'30''$ E, $25^{\circ}39'13''\sim 25^{\circ}41'00''$ N) (Figure 1). Karst landforms account for 87.92% of the total area, with a subtropical hot and dry valley climate, rain, and heat all co-occurring in time. The seasonal distribution of its precipitation is uneven, with most of the rain being concentrated within the period of May to October, accounting for 83% of the annual rainfall, for an average annual rainfall total of 1100 mm [29]. Its average annual temperature is 18.4°C , with hot and humid summers and autumns and warm and dry winters and springs. The sample area is 607–890 m above sea level. This area has strong karstification, abundant underground cracks, karst caves, and serious soil erosion. Its soil average thickness is only about 30 cm and its lithology is Middle Triassic dolomitic limestone.

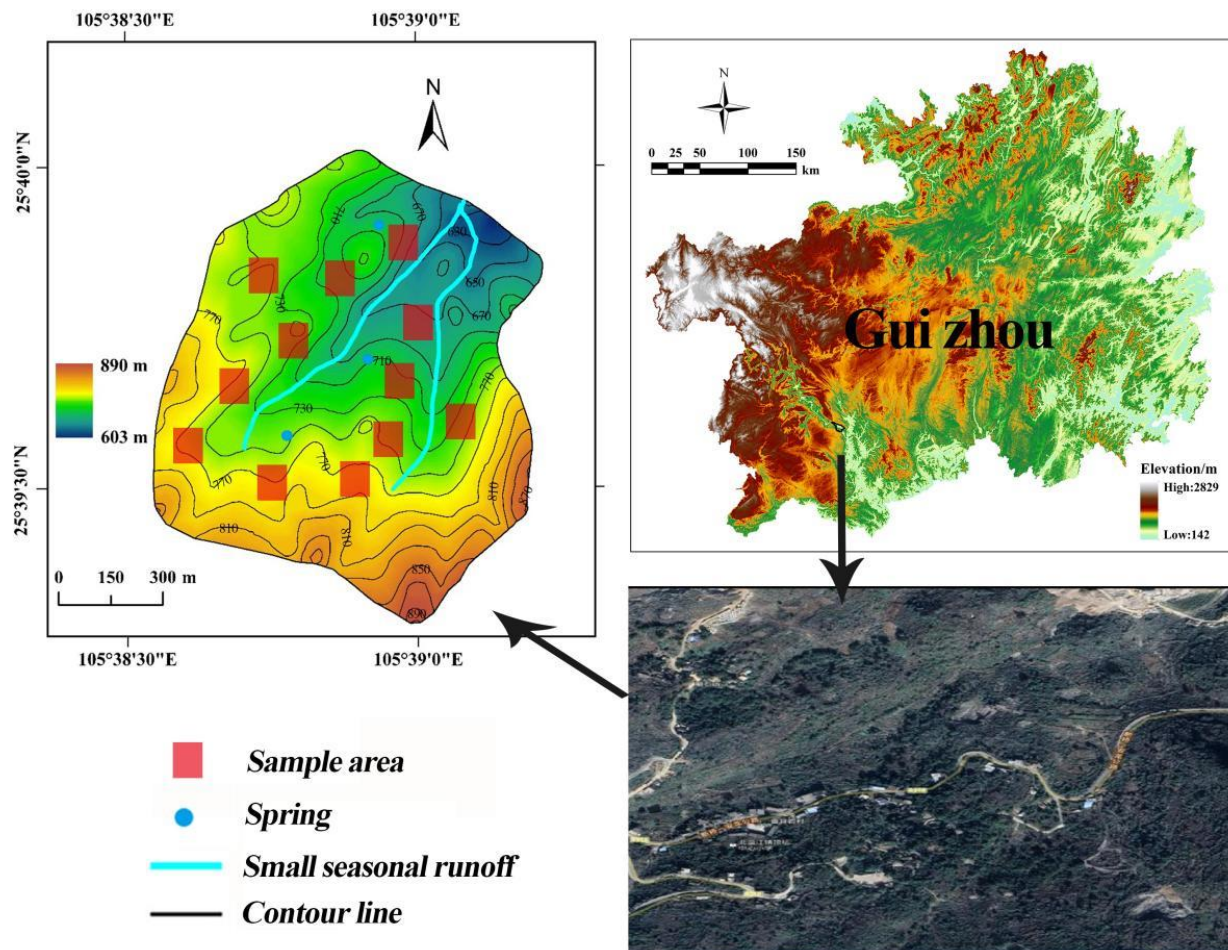


Figure 1. Geographical location of the study area. The left is a sampling point map, and the right is a regional satellite map. *Juglans regia*, *Zanthoxylum bungeanum* Maxim, *Eriobotrya japonica*, and *Lonicera japonica* these four plants are represented by their Chinese abbreviations in the following articles and charts, which are HT, HJ, PP, and JYH in the above order.

In the early 1970s, this area was a vast original forest with various types of vegetation, with the forest accounting for about 74% of the basin area. Subsequently, its artificial cultivation resulted in large-scale deforestation, with many plants recovering after a comprehensive conversion of farmland to forest in 2002. Nonetheless, the native vegetation

in the region has been seriously degraded, and the land is now occupied by secondary vegetation, mainly broadleaved forest, coniferous and broad-leaved mixed forest, and shrub. Its land use types are agricultural land and abandoned forestland, etc. The study area is rich in plant species, including *Lonicera japonica*, *Eriobotrya japonica* Lindl, *Pinus massoniana* Lamb, *Hylocereus undulatus* Britt, *Zanthoxylum bungeanum* Maxim, *Juglans regia*, and *Broussonetia papyrifera*. Among them, *Juglans regia*, *Zanthoxylum bungeanum* Maxim, *Eriobotrya japonica*, and *Lonicera japonica* (these four plants are represented by their Chinese abbreviations in the following articles and charts, which are HT, HJ, PP, and JYH in the above order) are the dominant species, with the largest local planting scales; they not only exhibit a great adaptability to the karst environment, but also bring considerable economic benefits to local residents.

2.2. Experimental Design and Sampling Collection

At the start of the experiment, the team performed a preliminary survey of the main plant species within the area's forests. The results showed that HT, HJ, PP, and JYH had the highest coverage compared to other plant species. Therefore, these four plants were selected as samples. The team found 360 plants of these four species across the region. After a statistical analysis of their physiological characteristics, such as the plant size and growth years of the samples, according to the average level of samples, a total of 12 representative sample plots (10 m × 10 m) were selected. The numbers of the four plant species in each plot tended to be consistent, with 4–5 from each species, totaling 217 tree species. The sample trees were the same in age, and their physiological characteristics, such as tree height, base diameter, and DBH, were roughly similar. The soil, plant, and spring water samples were collected once in each of the following months: September 2021, January 2022, April 2022, and July 2022 (the study area was located in southwest China, which is affected by subtropical monsoons and has a dry and hot valley climate. January, April, July, and September fall in winter, spring, summer, and fall. There would be significant changes in the rainfall and plant growth within the study area. Therefore, this paper chose these four months for sampling, which could be more representative).

On each sampling date, two plants with a similar growth morphology were randomly selected from each sample plot as sample trees (Table 1). A sample of each plant's xylem was collected from all four sides of its canopy. To avoid an isotope fractionation of the xylem water and a contamination with isotopically enriched water, the phloem tissue of the branches was removed [30]. All the plant samples were cut into 3–4 cm segments, placed in a high-boric-acid glass bottle, sealed with polyethylene film, and kept frozen in the refrigerator (4 °C) until the isotopic analysis. The fully expanded leaves of at least 10 individuals from each plant species on three slopes were collected to produce one composite sample for a carbon isotopic composition analysis. The leaves were dried at 60 °C and ground into a uniform powder that was sieved through a 1 mm mesh for the analysis of the carbon isotopic composition.

Table 1. Basic information of sampled plant species.

Species	Family	Life Form	Height (m) (Mean ± SD)	DBH (cm)	Coverage Area (m ²)	Sample Number
<i>Juglans regia</i>	Walnut genus	Arbor	11.28 ± 3.19	21.48 ± 2.72	35.46 ± 5.31	49
<i>Zanthoxylum bungeanum</i> Maxim	Peppercorn genus	Small deciduous trees	3.39 ± 0.21	5.52 ± 0.11	5.83 ± 0.19	55
<i>Eriobotrya japonica</i> Lindl	Loquat genus	Small deciduous trees	2.76 ± 0.24	5.31 ± 0.13	2.86 ± 0.34	53
<i>Lonicera japonica</i>	Honeysuckle genus	Evergreen	0.89 ± 0.23	2.31 ± 1.31	4.33 ± 1.29	60

The soil samples were collected at the same time as the plant samples. On each sampling date, using a ring cutter, the soil samples were collected separately under each sampled tree at depths of 10, 20, 30, 40, 50, and 60 cm. The soil samples were divided into two parts: one part was stored in a freezer for the isotope analysis and the other was used to obtain the soil water content by weight (the subsequent soil moisture content is represented by “SWC” %). The root samples were collected at 10 cm intervals of depth, separated from the soil, and washed with water. The diameters and lengths of all the root segments within each 10 cm deep segment were measured with calipers and rulers to determine the root surface area within each segment. Fine roots with diameters of less than 0.001 m and roots with decayed surfaces were not recorded.

The surface of a karst area tends to be rugged and fragmented, with widespread fissures; as a result, fissure water is also a possible source of plant water. After a statistical survey of all the fissures in the region, the research team separately selected three representative fissures within the sampling area of each slope position. These fissures were located at an average distance of 2–3 m from the sample trees and had depths that varied from 0.4–1.5 m, and some plant roots extended to this point. Alternatively, either an underground water source that contributed to the pore leakage into a spring or the spring itself could be used [17]. Because a spring was located at each of the upper and middle slope positions, we also collected spring water in glass bottles and refrigerated these water samples. The fissure soil and spring samples were collected at the same time as the soil and plant samples, with a total of 72 fissure soil samples and 48 spring samples. The sampling time was similar to that of the plant soil. Because the water used to irrigate the HJ and PP was derived from precipitation, it was not separately included in this study.

In addition, a funnel device was used to collect the precipitation directly. The rainwater samples were also placed into glass bottles and sealed with film before the isotope analysis. The meteorological data were monitored over time by a small weather station in the study area (ATMOS, Meter Company, NC, USA). The equipment recorded the precipitation, air temperature, relative humidity, atmospheric pressure, and photosynthetically active radiation, at a frequency of 30 min per sampling record.

2.3. Isotopic Analysis

Water was extracted from the collected plant and soil samples using a low-temperature vacuum extraction instrument (LI-2100, LICA, Beijing, China), with the extraction process taking 2 to 3 h. Using this approach, the extraction efficiency exceeded 98%, which was sufficient for obtaining appropriate water samples [28]. The extracted water samples and rainwater samples were filtered through a 0.22 µm filter to eliminate any impurities and organic contaminants. Isotope measurements were performed on the filtered water samples using a liquid water isotope analyzer (TLWIA, Lijia, Beijing, China). The accuracy of the liquid water isotope analyzers for the $\delta^{18}\text{O}$ and $\delta^2\text{H}$ is usually better than 0.1‰ and 0.3‰, respectively [31]. Due to the spectral contamination of the water samples that were extracted at a low temperature, the spectra of the test results were corrected according to the instrument’s calibration procedure [32]. The weighted averages ($\delta_{p,mean}$) of the $\delta^2\text{H}$ and $\delta^{18}\text{O}$ in the monthly precipitation were calculated as follows:

$$\delta_{p,mean} = \frac{(\sum_{i=1}^n \delta_{p,i} \times PPT_i)}{(\sum_{i=1}^n PPT_i)} \quad (1)$$

where $\delta_{p,i}$ is the $\delta^{18}\text{O}$ and $\delta^2\text{H}$ of the i th precipitation event, and PPT_i is the amount of the i th precipitation.

2.4. MixSIAR Analysis

The stable isotopes of the xylem water were compared to those of the potential water sources, and the intersections of the two were then used as initial indications of the depth from which each plant was absorbing water. The current proportion of the water used by plants is usually estimated by the Bayesian mixing model MixSIAR (version 4.2.0),

which includes the uncertainties and discriminant factors that are associated with multiple water sources [33]. The initial xylem isotope values, $\delta^2\text{H}$ and $\delta^{18}\text{O}$, for the four plants were used as mixed data inputs for MixSIAR, and the means and standard errors of the isotope values ($\delta^2\text{H}$ and $\delta^{18}\text{O}$) at the different soil layers (0–10 cm, 10–20 cm, 20–30 cm, 30–40 cm, 40–50 cm, 50–60 cm, fissure water, and groundwater) were used as the source data within the MixSIAR program. There was no concentration dependence in the source data. Because isotope fractionation did not occur due to the plant water absorption, the discrimination data were set to zero [34]. The run length of the Markov chain Monte Carlo (MCMC) was set to 'long' (chain length = 300,000; burn = 200,000; thin = 100; and chains = 3). Gelman-Rubin and Geweke diagnostic tests were used to determine whether the model was close to convergence [33] and the model's predictions were expressed as the mean values. Previous sample surveys found that the soil layers in the study area were generally unevenly distributed and shallow; therefore, only the 0–60 cm soil samples were retrieved. When analyzing the soil water, the soil isotope values between the different soil layers at 0–60 cm of depth were not readily apparent, so the water sources from the different soil layers were combined into two larger layers (0–30 cm and 30–60 cm) to facilitate a subsequent analysis and comparison. The two layers were identified based on the following approach [22]:

- (1) The shallow layer (0–30 cm): The SWC and isotope values from the first 30 cm were close to each other, with a small variation along the vertical profile. In addition, the soil that resided close to the surface could easily be affected by rainfall and evaporation, so the soil water isotope value and SWC tended to exhibit a large range of variation between the seasons.
- (2) The deep layer (30–60 cm): The SWC and isotope values in this layer changed less than those in shallow soil, because the soil layer was deeper and thus less affected by external precipitation and evaporation. As a result, the changes between the seasons were smaller.

2.5. Data Analyses

A K-S was used to test the normality of all the parameter sets and a linear regression analysis was used to understand the relationship between the $\delta^{18}\text{O}$ and $\delta^2\text{H}$ of each plant and its potential water source. After a box plot detection, the outliers were removed and the best fitting line was drawn to determine the equation, R coefficient, and p value. The differences in the xylem water content's $\delta^{18}\text{O}$ and $\delta^2\text{H}$ at $p < 0.05$ were analyzed by a one-way ANOVA and minimum significance difference (LSD) analysis. Then, the differences in the soil water isotope composition of each plant in the same month and the significant differences in the water sources of the different plants, with seasonal variations, were detected by a post-Tukey test and the minimum significant difference. An IBM SPSS 23-line statistical analysis was used for all the data, and Excel 2019 and Origin 2018 were used for the data editing and visualization.

3. Results

3.1. Precipitation Distribution and Isotopic Composition

The precipitation and temperature in the study area from August 2020 to July 2022 are shown in Figure 2, revealing a daily rainfall that ranged from 0 mm to 76 mm. Throughout the rainy season, a total of 1197.96 mm of rainfall occurred, accounting for 81.7% of the annual precipitation, of which the highest monthly rainfall was recorded at 283.4 mm in June. This latter value alone accounted for 19.33% of the annual total rainfall. The average daily rainfall was 6.65 mm during the rainy season and only 1.48 mm during the dry season. The daily temperature ranged from 4.16 °C to 30.98 °C and the average temperatures during the rainy season and dry season were 24.84 °C and 14.73 °C, respectively. In comparison, the rainfall increased by 10.11% in 2022 compared to 2021 (Figure 2).

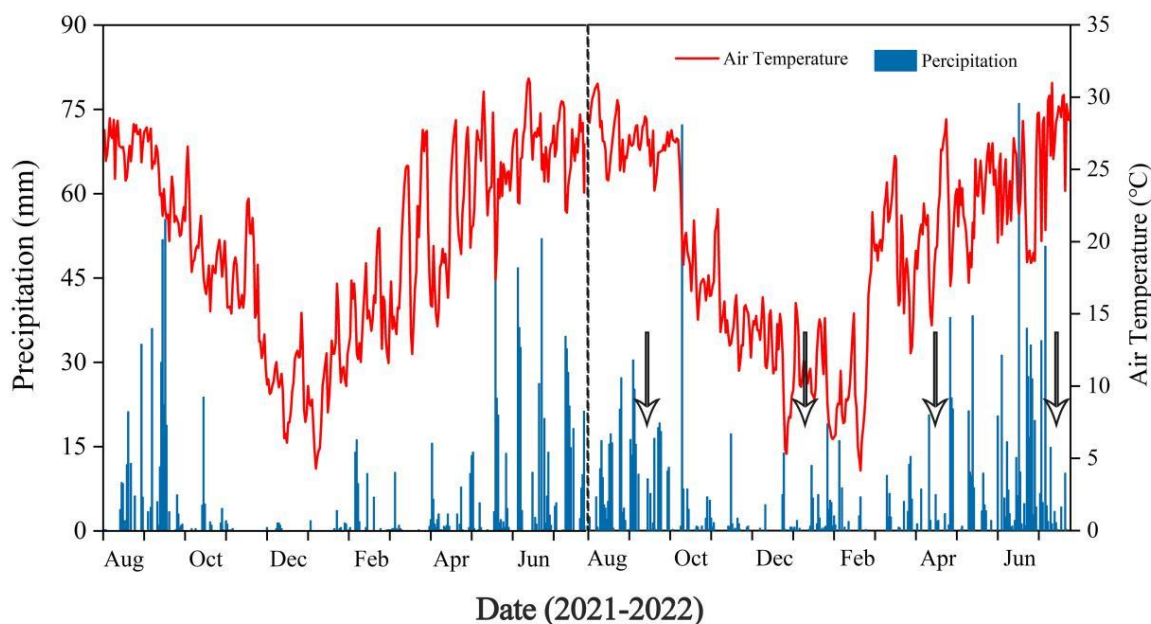


Figure 2. Precipitation and temperature in the study area from August 2020 to August 2022. The black arrow in the figure represents the sampling date.

The isotopic composition of the precipitation showed great changes during the sampling period, with the $\delta^{18}\text{O}$ ranging from -5.15‰ to -11.36‰ , with an average of -7.57‰ . The range of the $\delta^2\text{H}$ was -37.41‰ to -83.51‰ , with an average of -60.48‰ (Figure 3). The local atmospheric precipitation line (LMWL), which was fitted according to the precipitation data (Figure 4), showed that the slope and intercept of the LMWL were smaller than those of the global atmospheric precipitation line (GMWL) [35]. The isotope values of the four plants mostly fell to the right of the LMWL, meaning that the soil water came from rain and underwent a degree of evaporation. It can also be seen from the soil water line (SWL) for the different slope positions of the four plants that the soil water source within each soil layer was precipitation (Figure 4).

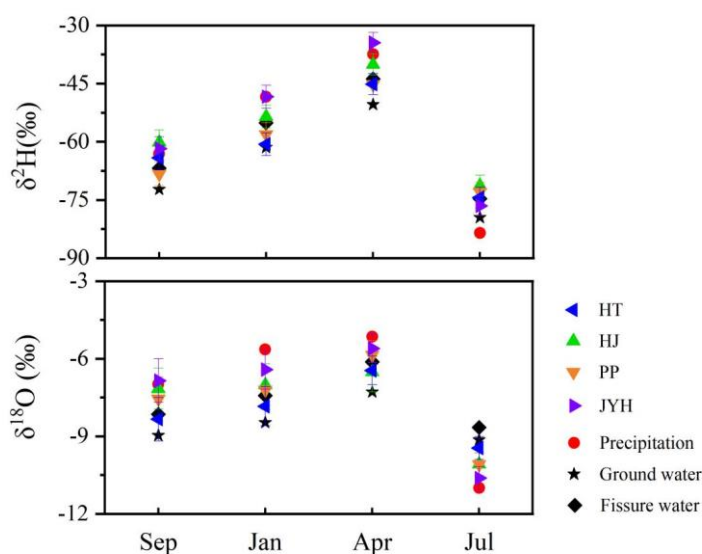


Figure 3. Seasonal variation of $\delta^2\text{H}$ and $\delta^{18}\text{O}$ values in xylem water of different water bodies and four plant species. The error bar represents the standard deviation. The $\delta^2\text{H}$ and $\delta^{18}\text{O}$ in rainwater represent the values of weighted averages per month.

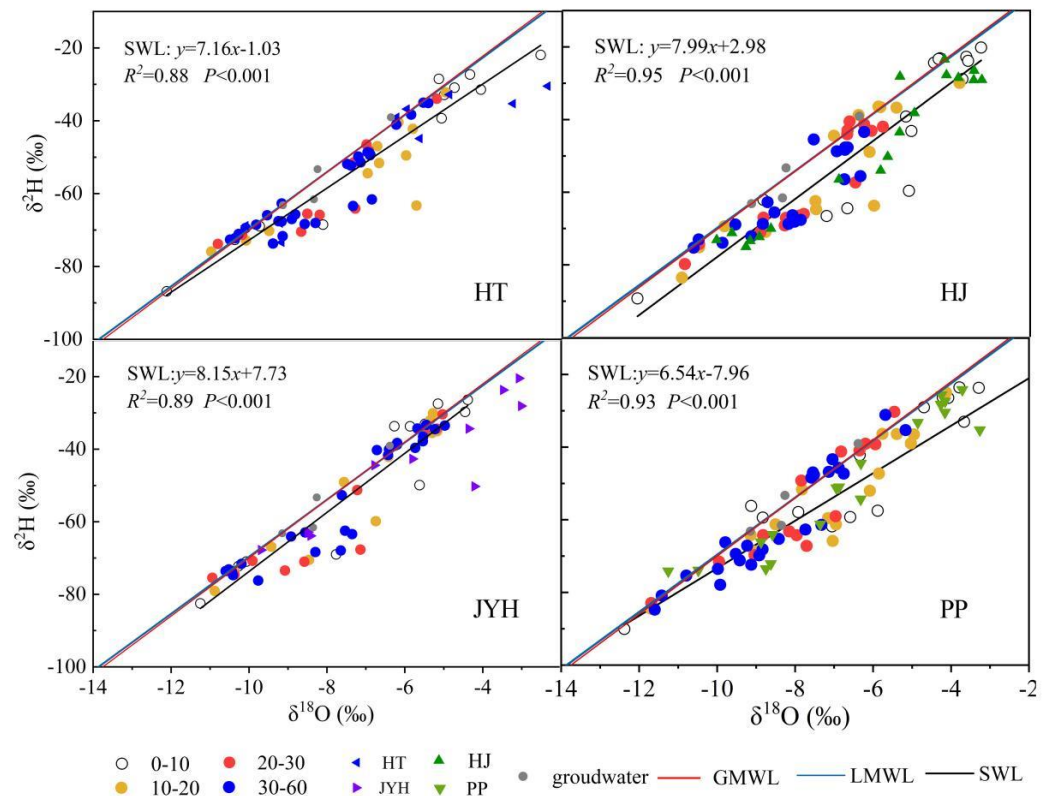


Figure 4. The linear regression relationship between $\delta^2\text{H}$ and $\delta^{18}\text{O}$ of soil moisture of four plant species in the study area. SWL represents soil water line based on isotopic data of soil water. LMWL represents the local meteoric water line ($y = 7.86x + 9.02$, $R^2 = 0.98$, and $p < 0.01$). GMWL is the global meteoric water line ($y = 8x + 10$) [35]. LMWL and GMWL are plotted in each panel for reference. The isotopic compositions of xylem water from four species are shown in the Figure 4.

3.2. Isotopic Composition and Variation of Xylem Water

The isotopic values of the xylem water varied with the sampling time and species. For HT, the $\delta^2\text{H}$ ranged from -46.37‰ to -77.24‰ and the $\delta^{18}\text{O}$ ranged from -6.42‰ to -10.22‰ ; for the HJ, the $\delta^2\text{H}$ ranged from -38.85‰ to -76.34‰ and the $\delta^{18}\text{O}$ ranged from -5.72‰ to -10.22‰ ; for the PP, the $\delta^2\text{H}$ values of the loquat ranged from -41.24‰ to -79.99‰ and the $\delta^{18}\text{O}$ values ranged from -5.85‰ to -10.69‰ . The variation ranges of the $\delta^2\text{H}$ and $\delta^{18}\text{O}$ of JYH were the largest (Figure 3) and it is speculated that the water source of JYH was shallow and most affected by the surface rainfall evaporation. Overall, there was no significant difference between HJ and PP ($p > 0.05$) when averaging the xylem water isotope values across all the sampling dates, suggesting that both species were absorbing water from similar soil layers. However, the analysis on the sampling dates showed that the four planting covers had significant differences between the seasons ($p < 0.05$), indicating that the water absorption of the plants had an obvious time variability. From September 2021 to July 2022, the $\delta^2\text{H}$ and $\delta^{18}\text{O}$ in the xylem water of the four plants increased first and then decreased, and the change trend was basically the same, with the maximum value appearing in April and the minimum value in July (Figure 3). Meanwhile, the isotopic composition of HT and HJ was close to the fractured water and 30–60 cm water source in most cases, and occasionally close to the groundwater and precipitation, while the honeysuckle mainly depended on the 0–30 cm surface soil water and precipitation, and PP changed significantly between the deep and shallow water sources (Figure 3). In combination with Figure 4, the isotopic values of the plant xylem water were distributed across the different soil layers, indicating that soil water was still the main source of water for all four species. Among them, the water utilization of HJ and PP was very similar.

3.3. Soil Moisture and Isotopic Composition

The soil moisture's $\delta^2\text{H}$ and $\delta^{18}\text{O}$ experienced significant seasonal variations by depth and month (Figures 4 and 5). Because the soil layers in karst areas are shallow, there was no significant difference in the soil water content in the upper 0–30 cm soil layer (0–10, 10–20, and 20–30) depth in the vertical section ($p > 0.05$), and the variation value within a single season was only about $\pm 4\%$. The SWC of the HT, HJ, and PP samples showed a similar trend at each depth. The water content of all the soil layers gradually increased from 0–40 cm and showed a turning point from 40 cm (Figure 4), gradually decreasing or increasing slowly. This may be because 0–40 cm was greatly affected by the surface rainfall, and the soil thickness in karst areas is generally about 40 cm. Further down, it is difficult to store precipitation due to the influence of gravel and cracks, etc., and the distribution being extremely uneven. In different months, the soil water content in the rainy season was generally higher than that in the dry season, with the lowest occurring in January and April and the highest in July. In July, the soil water content of HT reached 37.15%, which was the best water-retaining species among the four plants; HJ and PP followed, reaching 36.08% and 35.76%. The lowest SWCs of HT, HJ, PP, and JYH were 27.24%, 26.15%, 24.10%, and 24.06%, respectively. During the sampling period, the SWC in the shallow soil layer (0–30 cm) changed more than that in the other soil layers, while the SWC in the deep soil layer (30–60 cm) was relatively stable, and the same trend was observed for all four species.

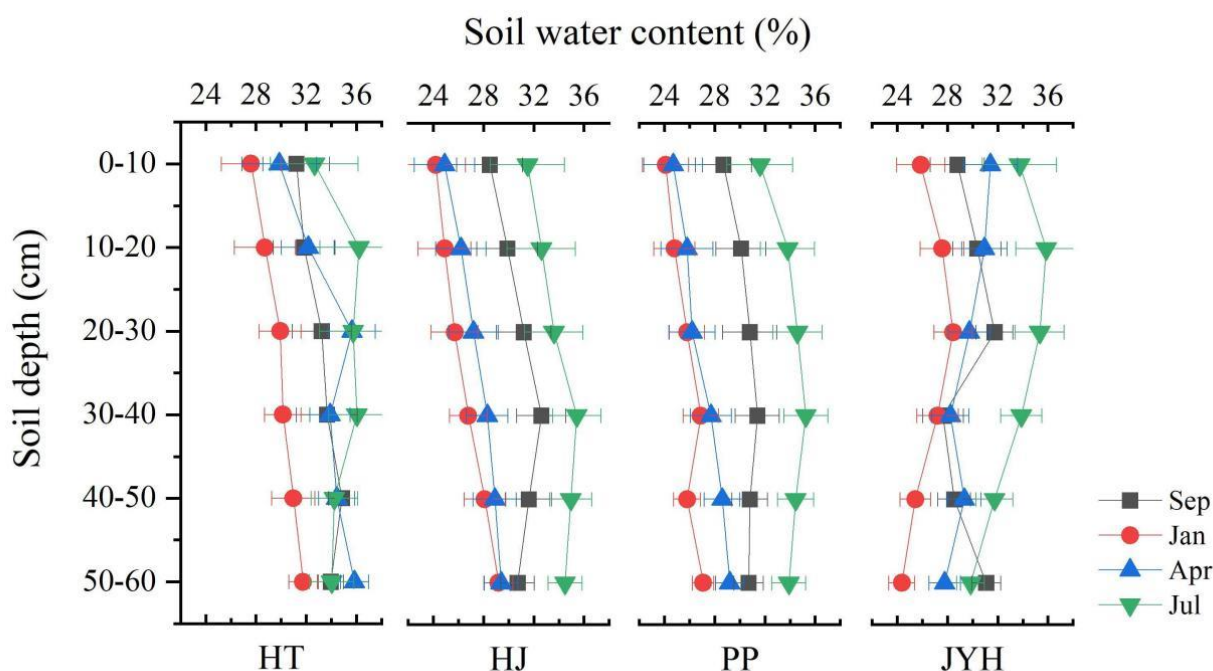


Figure 5. Changes in soil water content between HT, HJ, PP, and JYH in 0–60 cm section. The error bar represents the standard deviation.

The isotopic composition of the soil water varied with the soil depth and plant species. During the sampling period, the isotopic composition of the soil water became poorer as the soil depth increased, and the difference in the isotopic values and variations in the shallow soil water (0–30 cm) was higher than that in the deep soil water (30–60 cm). From a seasonal point of view, there was no significant difference between the shallow and deep soil water isotopic compositions of HJ and PP ($p > 0.05$). The $\delta^2\text{H}$ and $\delta^{18}\text{O}$ values of HT ranged from -21.94‰ to 86.83‰ , and from -2.55‰ to 12.21‰ , respectively. The $\delta^2\text{H}$ and $\delta^{18}\text{O}$ values of HJ ranged from -32.17‰ to 77.34‰ , and from -5.04‰ to 10.91‰ , respectively. Those of PP ranged from -31.41‰ to -77.76‰ and -5.26‰ to 9.59‰ , while those of JYH ranged from -3.26‰ to -11.25‰ and -20.87‰ to -82.51‰ , respectively.

From January to July, the $\delta^2\text{H}$ and $\delta^{18}\text{O}$ in the xylem water of the four species decreased gradually and increased in September (Figure 3).

3.4. Variations in the Proportion of Plant Water Uptake

According to the graph inference method, the isotopic ratios of the xylem water, crack water, and soil water of the four plants overlapped at several soil depths during the study period (Figures 6 and 7), suggesting that the plants could obtain water from several sources. Using the MixSIAR model further to predict the water absorption ratios of the plants, HT mainly depended on 30–60 cm deep water sources ($41.8 \pm 6.86\%$) and crack water ($32.5 \pm 4.21\%$) during the rainy season in July and September, while its use of surface water sources 0–30 cm ($22.5 \pm 2.86\%$) was relatively small (Figure 8). This was related to the sufficient precipitation during the rainy season, which increased the water content of the surface layer (Figure 5), while the dry season mainly relied on deep and fissure water. For HJ during the dry season, deep soil water was dominant ($45.24 \pm 4.16\%$) and shallow soil water was secondary ($25.5 \pm 4.38\%$). However, in the rainy season, the water source was mainly shallow soil water ($45.6 \pm 3.94\%$), which was supplemented by deep soil water ($22.03 \pm 4.22\%$).

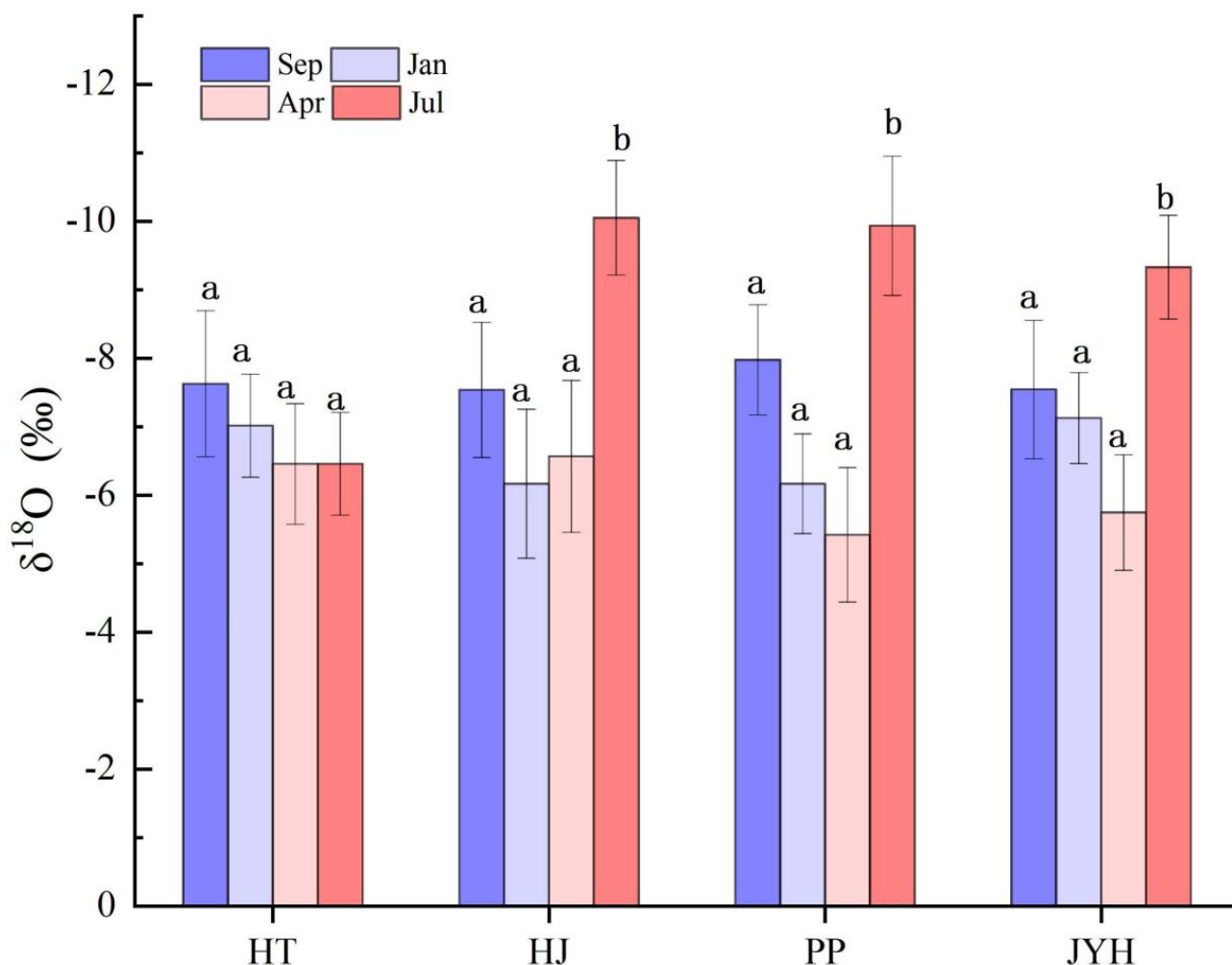


Figure 6. Significant differences in soil water isotope composition of four plants in the same month. a and b represent different significant differences. Error bars represent standard deviations, $p < 0.05$.

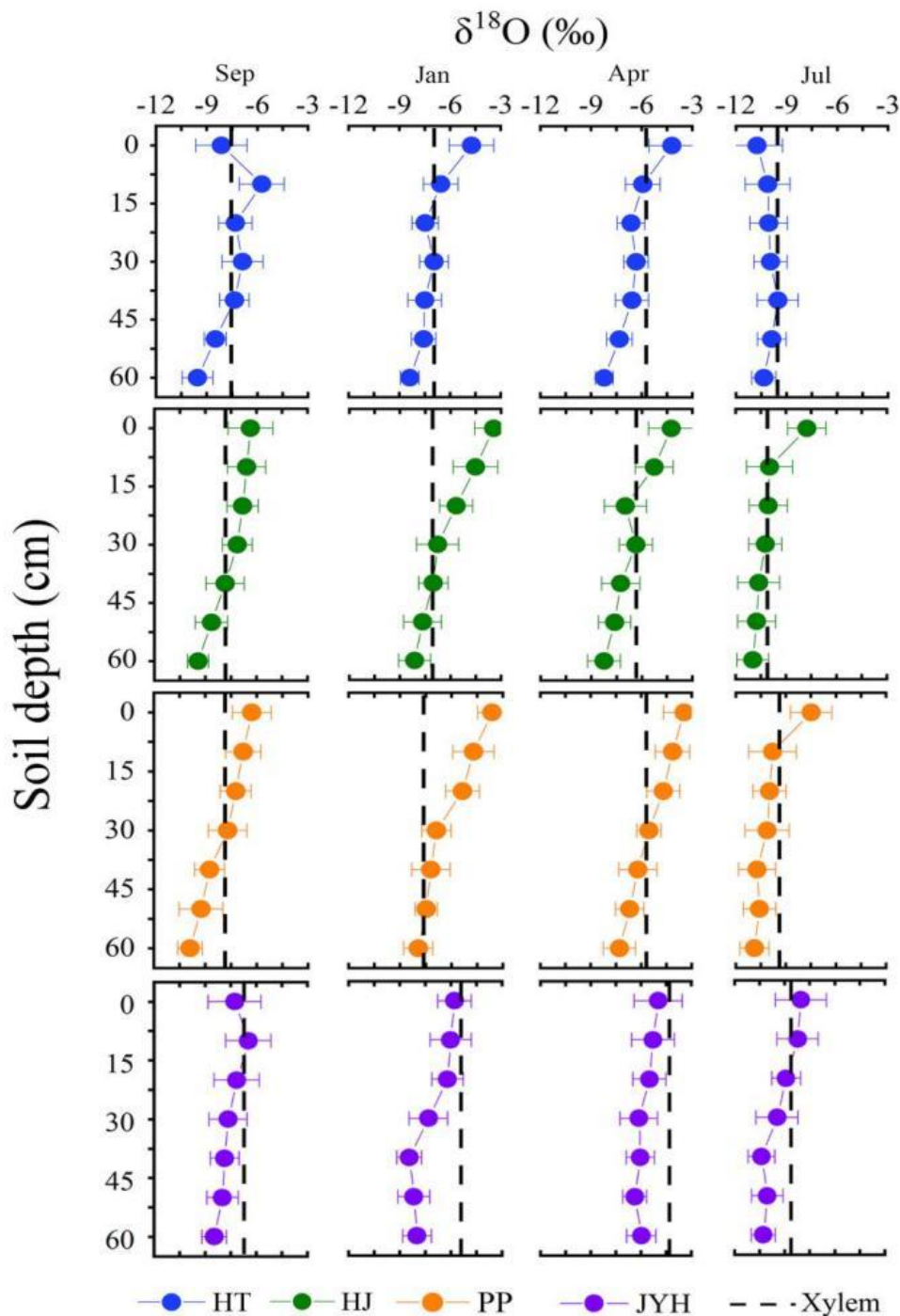


Figure 7. Seasonal variation in $\delta^{18}\text{O}$ in soil layer (0–60 cm) and xylem water (vertical dashed line) of four species. From left to right are September 2021, and January, April, and July 2022. Error bars represent standard deviations ($p < 0.05$).

In contrast, the water absorption pattern of PP was the same, and the difference was only slightly different in numerical value (Figure 8); for example, the absorption of shallow water in the rainy season reached $54.31 \pm 3.36\%$, while that in the dry season was only $12.53 \pm 4.24\%$ (Figure 8). In contrast, the water absorption ratio of JYH was significantly different, as JYH was dominated by 0–30 cm surface water (61.3%) in both the dry and rainy seasons (Figure 8). Individual plants may have also reached as deep as 40 cm into the water, which was mainly related to JYH's root system. In addition, the proportion of water sources for HT was relatively balanced and the change was slightly small, as the main body of HT

relied on a 30–60 cm water source and fissure water ($70 \pm 3.22\%$) (Figure 8). HJ and PP transferred flexibly between the shallow layer during the rainy season and the deep layer during the dry season, and it can also be clearly seen from Table 2 that the proportion of the water sources in the loquat varied significantly between the seasons. During the sampling period, there was no significant difference in the water absorption patterns between HJ and PP ($p > 0.05$), but there was a difference in the water absorption ratio between the seasons ($p < 0.05$), as shown in Table 2. The utilization of shallow water by JYH was significantly higher than that by the other plants in the dry rainy season, and the utilization of deep water from 30–60 cm by the other three plants was significantly higher than that by JYH in the dry rainy season.

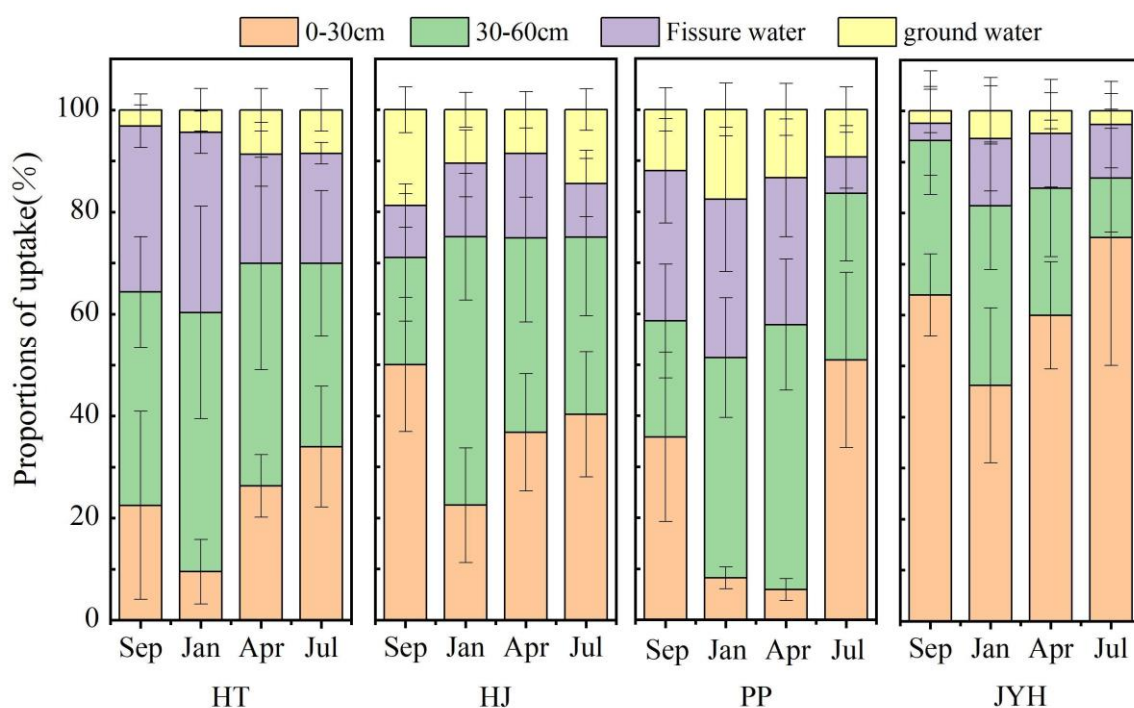


Figure 8. Seasonal variations in proportion of water uptake from different soil layers based on MixSIAR for HT, HJ, PP, and JYH. Error bars represent standard deviation.

Table 2. Changes in water use ratio of four species in dry rainy season.

Water Source Plants	<i>Juglans regia</i>		<i>Zanthoxylum bungeanum Maxim</i>		<i>Eriobotrya japonica Lindl</i>		<i>Lonicera japonica</i>	
	Dry	Rainy	Dry	Rainy	Dry	Rainy	Dry	Rainy
0–30 cm	17.9% ^c	28.3% ^c	29.6% ^b	45.2% ^b	7.1% ^d	43.4% ^b	53.1% ^a	69.6% ^a
30–60 cm	47.2% ^a	38.9% ^a	45.4% ^a	27.8% ^b	47.6% ^a	27.7% ^b	30.1% ^b	20.9% ^c
Fissure water	28.4% ^a	27.1% ^a	15.5% ^b	10.4% ^c	29.9% ^a	18.3% ^b	12.0% ^b	6.9% ^c
Ground water	6.6% ^b	5.9% ^b	9.6% ^b	16.7% ^a	15.5% ^a	10.6% ^a	4.9% ^b	2.6% ^b

By contrast, in the table, ^a, ^b, ^c, and ^d represent the significant difference in water utilization ratio of the four plants in the same season, $p < 0.05$.

3.5. Changes of Carbon Isotopes in Plant Leaves

The seasonal variation in the $\delta^{13}\text{C}$ in the leaves of the four plant species was measured during the study period. The results showed that leaf $\delta^{13}\text{C}$ of the four planting species changed from high to low from the dry season to the rainy season (Figure 9). Under drought conditions in January, the $\delta^{13}\text{C}$ was generally high, and HJ and HT were the highest, at -26.24% and -26.37% , respectively. In the rainy season, the $\delta^{13}\text{C}$ values were generally low, especially in July, when the precipitation was sufficient and the plants were not affected

by drought stress, adopting a low water use efficiency (Figure 9). The WUE of each plant species was at a low level. In addition, by analyzing the $\delta^{13}\text{C}$ value, HT, HJ, and PP, in descending order, were $\text{HT} > \text{HJ} > \text{PP}$. This is the same as the result that was obtained in Figure 8, where HT and HJ had a higher water use efficiency and higher survival rate than the other two species.

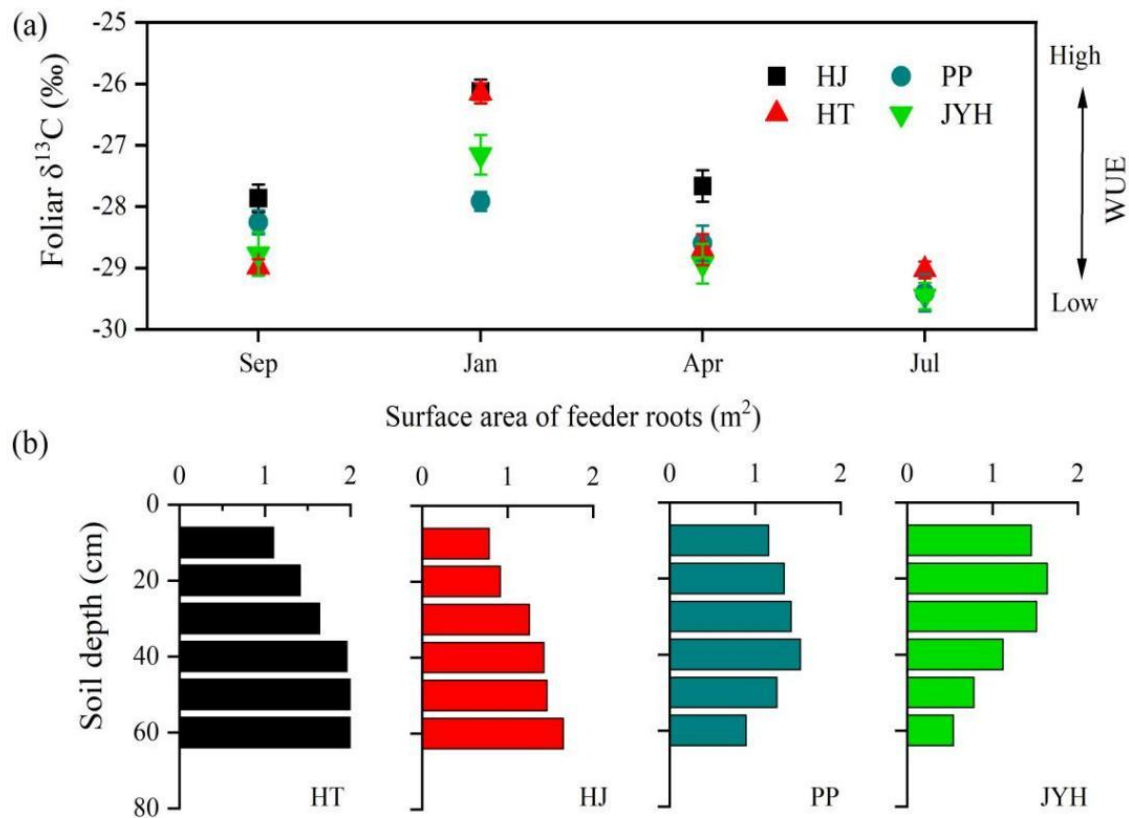


Figure 9. (a) Seasonal variation of $\delta^{13}\text{C}$ values in leaves of HT, HJ, PP, and JYH. (b) Profile distribution of root surface area of four species. Error bars represents standard error.

4. Discussion

4.1. Vertical Gradients of Forest Soil Water Isotopic Composition

In subtropical forests, the vertical gradient of soil water isotopes is mainly affected by evaporation and infiltration, as well as the mixing of old and new rainwater [36]. It could be clearly seen that 0–60 cm, from the surface to the deep layer, presented a clear trend of gradual depletion. It only showed significant changes at about 0–15 cm, because it was close to the surface and was greatly affected by precipitation and evaporation. The further down the soil was, the less the external precipitation evaporation had an influence, so the water isotope of deep soil tended to be stable. The stable isotope ratios of the four plants from 0–60 cm decreased, as shown in Figure 7. As the authors make clear, there was no significant difference between the different months and different depths among some plants (HJ and PP), as only the range and trend of the variation were described. Due to the small data gap, the data analysis showed that there was no statistically significant difference (Figures 6 and 7). As the soil depth increased, the $\delta^2\text{H}$ and $\delta^{18}\text{O}$ in the soil moisture became more depleted. Compared to the deeper soil profiles in January and April, the isotopic composition in the surface 0–30 cm soil water was more abundant (Figures 6 and 7). This is attributed to the decreased rainfall and increased evaporation in the surface soil layer [37]. However, due to the influence of rainfall with poor isotopic values in the summer, this trend was reversed in the topsoil during July and September, suggesting that precipitation was also an important factor controlling the soil water isotopic composition [22,38,39]. The

isotopic ratios of the surface soil displayed larger variances than those of the deep soil, due to the combined influences of evaporation and precipitation. In this study, the $\delta^{18}\text{O}$ values of the 30–60 cm soil changed less by depth and sampling date than those of the 0–30 cm soil (Figures 6 and 7). HJ and PP showed the same change pattern, suggesting that the influence of evaporation on the deep soil was limited [36,40]. The fissure water in the study area often came from rainwater that had seeped into the soil, and the vertical changes in the soil isotope composition were caused by the mixing old and new water [41,42], which would then infiltrate into the deeper soil layers [43].

The isotopes in precipitation generally show the seasonal variation characteristics of being low in summer and high in winter, which is mainly related to the water vapor sources in the winter and summer half years and the meteorological conditions during precipitation [17,28,44]. In the summer half year, southwest China is mainly affected by the oceanic warm and humid air masses of southwest monsoons and southeast monsoons, with sufficient water vapor, a high humidity, and weak evaporation [44]. According to the Rayleigh fractionation principle, the heavy isotopes in precipitation would be depleted with a decrease in the water vapor content during the transport process of air mass, and the $\delta^{18}\text{O}$ would be low. In the winter half year, the region is mainly affected by the westerly dry and cold water vapor mass and the local evaporation of water vapor, with the water vapor content being low, the air being relatively dry, the evaporation being strong, the heavy isotope being gradually enriched in precipitation, and the $\delta^{18}\text{O}$ being high [45,46]. Compared to the GMWL, the slope and intercept of the atmospheric precipitation line in the study area were relatively small, indicating that the climate in this region is warm and humid, that there is a certain degree of secondary evaporation in the precipitation process, and that the unbalanced evaporation effect is larger. This is mainly related to the temperature of the water vapor condensation, the evaporation conditions, the water vapor source, and the transportation mode [46].

4.2. Differences in Seasonal Water Uptake Patterns among Species

According to the regression diagram of the soil water's $\delta^2\text{H}$ and $\delta^{18}\text{O}$ in Figure 4, the xylem isotopic compositions of the four plants were distributed in 0–60 cm of the soil and water, suggesting that most of the water sources for the subtropical forest plants during the study period came from the 0–60 cm soil layer [47]. Figure 8 also shows that about 71.67% of the water sources for the four plants came from 0–60 cm of the soil water. During the study period, HJ and PP were concentrated in deep water absorption during the dry season and shallow water absorption during the rainy season. HT, however, was always dominated by deep water sources and fissure water sources, and the reason for this was that the three plants belonged to different functional types. As a macrophanerophytes, HT has numerous root systems and goes deep underground, so it can use deep water sources and water that is stored in rock cracks with great efficiency [48]. As small trees and shrubs, HJ and PP have small and shallow roots, and, in order to achieve a higher water use efficiency, their absorbed water sources can be flexibly converted between deep and shallow layers. In a study of aspen and other plants, Flanagan et al. also found that plants not only absorb soil water, but also involve groundwater [49]. It could be seen that the water absorption patterns of HJ and PP showed the same “dimorphic root system” [48,50,51], which indicates that their water resource utilization had a certain plasticity level. Wang et al. found that Huangjing could switch between deep and shallow water sources with seasonal changes, which was similar to our experimental results [47].

In contrast, JYH's water absorption was more extreme between the seasons, with the difference between the dry season and rainy season in the 0–30 cm soil layer being only about 16.7% (Figure 8). The contribution ratio of the water absorption was significantly different from that of the other three plants ($p < 0.05$). Karakis and other researchers found in their experiments on grape that the depth of a vine's water-absorbing root system could vary over time. Shallow roots used rainwater as their main source during spring, and with the advance of the growing season, the roots could gradually penetrate into the soil

profile [52]. Similar results have been found for other ecosystems [25,53], and shrubs or small trees will gradually increase their water absorption depth during the growing season. This also had some similarity to our study, but it remains to be seen whether the roots of plants gradually infiltrated into the soil layers with the growing season, due to a lack of data [54,55]. In addition, although both belong to the “dimorphic root system”, PP still showed different characteristics to HJ, as its water source segmentation was more severe during the dry season and the rainy season (Figure 8), which may be related to the root systems of both [56,57]. At the same time, during a precipitation event in July, PP was greatly affected by precipitation [58], and the contribution ratio of the surface water increased rapidly (Figure 8), while that of the deep water decreased slightly. However, HJ is relatively slow and its rise is not obvious. This is influenced by the root system of HJ, as, compared to PP, the root system of HJ has a deeper distribution and fewer fibrous roots on the surface, which is less responsive to surface rainfall (Figure 9).

The four plants, all belonging to subtropical forest vegetation, showed different levels of ecological plasticity under the same precipitation conditions. The shallow root system of PP, coupled with small evergreen trees, resulted in a low plasticity level for its water resource utilization [56,59]. Especially during dry years, many cases of dry death occurred when there was no rain for a long time [13]. Furthermore, both PP and HJ belong to small trees and have similar water use patterns, meaning that water competition exists between these species. Adequate water sources during the rainy season can ensure the survival of both, but under severe water stress, PP will be more passive [58]. Zhang et al. found that, in plants from subalpine habitats that mainly absorb water from the surface layer (0–30 cm), subalpine shrubs compete for water resources at similar depths during the drought and growing seasons, with a high water demand, resulting in plant dieback [60].

4.3. Hydrological Niche Separation and Ecohydrological Regulation of Forest Vegetation

During the dry season and rainy season, the water source of each plant in the same habitat of a subtropical forest is different. With a change in water conditions, their water use strategies will also change, showing a greater drought tolerance [12,15,61]. In this study, HT, as a deciduous tree with stout branches and deep roots, had the same water use pattern in both the rainy and dry seasons, with soil water of a 30–60 cm depth and fissure water always being its main sources (Figure 7). Thus, in the dry season, HT would compete for water with HJ and PP within the same lifetime. Moreover, HJ and PP had the same water use pattern, indicating that they would compete for water resources at a similar depth. With a small body size and shallow root system, the latter showed obvious weakness in its water absorption [62]. In the rainy season, with sufficient precipitation, HJ and PP turned to the shallow water source of 0–30 cm, while HT was still dominated by the deep water, so there was no competition between them and a clear separation of hydrological niche. However, as a perennial semi-evergreen shrub, the root system of JYH was mainly concentrated at around 0–40 cm (Figure 8) and its water resources throughout the whole year came from this. It was in competition with HJ and PP, and the water use capacity of the three factors determined the survival status of the species, with HJ usually winning. It follows that there are complex water use patterns among plants within the same lifetime of these subtropical forests. HT competed with HJ and PP during the dry season and HJ and PP competed with JYH during the rainy season, while HJ competed with PP all the time. JYH and HT were in a state of hydrologic niche separation, and they did not pose a threat to each other; therefore, large swaths of JYH were often seen growing around HT in the study area. The hydroecological niche isolation (HNS) hypothesis proposes that, within a community, plants may differ in their hydraulic characteristics in order to avoid or tolerate drought along the water availability gradients, thus avoiding competition [23]. These features include water absorption (e.g., different rooting depths or possibly leaf water absorption), differences in their stomatal control, and differences in their xylem structures [63]. The four plants in this study belong to different functional types of vegetation, with significant differences in their plant sizes.

The root depth of HT was much greater than that of the other three species, so it could utilize deeper water. Deciduous trees reduce water evaporation during the dry season and greatly improve their water use efficiency. In fact, these characteristics can have a significant impact on hydrological processes [64].

Previous studies have shown that tree size is also related to effective rooting depth [65] and demonstrated that this interdependence is related to different hydraulic strategies. Rooting depth increases with tree height, compensating for the greater evaporation requirements at the top of the canopy [66] and allowing larger trees to be photosynthetically active during the dry season. Our data in this study show a coordination between the rooting depth and water absorption sources in seasonal subtropical forests, suggesting a trade-off between drought avoidance (i.e., deep roots) and drought tolerance [64,67]. Drought-resistant species are characterized by their deep roots, such as tall trees and shrubs, which enable the plants to survive close to the hydraulic safety limit [68,69]. This is the main strategy of most vegetation within a forest, and these complementary strategies allow for a niche partitioning within forest ecosystems and influence the structure of the dominant species in communities that are driven by water resources and light [70]. At the surface, trees take advantage of the abundant sunlight in the upper layers, shrubs take advantage of the weaker light in the middle layers, and herbs gather at the ground level. In the underground space, plant roots are interwoven layer by layer to gather soil nutrients on the one hand, and prevent soil erosion on the other. This is especially evident in the above-ground and subsurface binary structure space, with serious leakage in southwest karst areas [21]. Due to the community structure of forest vegetation, it is highly possible to gather precipitation and facilitate the successful completion of the forest ecohydrological process between the atmosphere, vegetation, and soil. The dense canopy in a forest system can reduce the flushing of the surface soil through rain [71], accumulate soil nutrients, further promote vegetation growth during the dry season, and increase productivity [72,73].

Due to the limited availability of soil water, plants during the drought and rain seasons are subjected to different levels of water stress [74,75]. Plants in hot, dry river valleys respond to drought in different ways. One way is that some deciduous species drop their leaves to reduce transpiration and remain dormant throughout the drought; another way is through changing the water absorption strategy according to the available water source [22]. HJ is not only a small deciduous tree, but also has a dimorphic root system, which can stably change its water source pattern between the seasons. This flexible water use strategy can greatly improve its survival rate [19]. Although PP also has a dimorphic root system, it also has a shallow root system, making it difficult for it to penetrate deeper and thus relatively dependent on shallow soil water [58]. This extreme shallow and deep water conversion between the seasons indicates its high dependence on the water environment. Moreover, as an evergreen tree [56], PP has a greater need for water [76], which makes it more likely to die than prickly ash in the same habitat.

5. Conclusions

In this study, we used a Bayesian mixing model (MixSIAR) combined with stable isotopes of hydrogen ($\delta^2\text{H}$) and oxygen ($\delta^{18}\text{O}$) to investigate the seasonal variations in the water uptake patterns of four plantations in a karst subtropical forest. The soil water isotopic composition varied in gradient along the vertical direction, and the variation in the soil water isotopic composition was greater in the shallow layer than in the deep layer. HT mainly relied on deep soil water and fissure water, while JYH mainly relied on shallow water. They did not compete with each other for water, but had a seasonal hydrologic niche separation from the other two species, which reduced the water competition. The stony desertification intensity in the study area was relatively high and there were a variety of vegetation types within the subtropical artificial forest, which led to water competition among the various species with the same water use pattern. The result of this inter-species competition led to plant drying and death. A reasonable species combination (for example, the deep planting of PP, with timely irrigation during the dry season; HT, HJ, and PP being

as far away from each other as possible; the adoption of grass irrigation, Joe irrigation, Joe grass, and other planting methods) would facilitate their symbiosis with each other. Staggered water uptake would greatly improve the survival of species and their adaptation to changing future environments, maintain the hydrological cycle of forest ecosystems, promote the transfer of water between the atmosphere, vegetation, and soil, and help the ecological restoration of karst areas. This study provides a method for determining more efficient plant combinations for karst forest vegetation habitats, and its results will have important implications for ecosystem vegetation restoration.

Author Contributions: Conceptualization, K.X.; methodology, B.F., Z.L.; software, B.F.; formal analysis, B.F.; writing—original draft preparation, B.F.; writing—review and editing, B.F., K.X.; visualization, B.F.; supervision, K.X., Z.L.; project administration, K.X., Z.L.; funding acquisition, K.X. All authors have read and agreed to the published version of the manuscript.

Funding: This study was supported by the Science and Technology Program of Guizhou Province (No. 5411 2017 Qiankehe Pingtai Rencai), the China Overseas Expertise Introduction Program for Discipline Innovation (No. D17016) and the National Major Research and Development Program of China (2016YFC0502607).

Institutional Review Board Statement: Not applicable.

Informed Consent Statement: Not applicable.

Data Availability Statement: Not applicable.

Conflicts of Interest: The authors declare no conflict of interest.

References

- Forzieri, G.; Miralles, D.G.; Ciais, P.; Alkama, R.; Ryu, Y.; Duveiller, G.; Cescatti, A. Increased control of vegetation on global terrestrial energy fluxes. *Nat. Clim. Change* **2020**, *10*, 356–362. [[CrossRef](#)]
- Brandt, M.; Yue, Y.; Wigneron, J.P.; Tong, X.; Tian, F.; Jepsen, M.R.; Fensholt, R. Satellite-observed major greening and biomass increase in south China karst during recent decade. *Earth's Future* **2018**, *6*, 1017–1028. [[CrossRef](#)]
- Konapala, G.; Mishra, A.K.; Wada, Y. Climate change will affect global water availability through compounding changes in seasonal precipitation and evaporation. *Nat. Commun.* **2020**, *11*, 3044. [[CrossRef](#)]
- Yang, X.-D.; Wu, N.-C.; Gong, X.-W. Plant Adaptation to Extreme Environments in Drylands. *Forests* **2023**, *14*, 390. [[CrossRef](#)]
- Yang, H.B.; Yang, D.W. Derivation of climate elasticity of runoff to assess the effects of climate change on annual runoff. *Water Resour.* **2011**, *47*. [[CrossRef](#)]
- Wang, J.; Fu, B.J.; Wang, L.X. Water use characteristics of the common tree species in different plantation types in the Loess Plateau of China. *Agric. For. Meteorol.* **2020**, *288–289*, 108020. [[CrossRef](#)]
- Bode, S.; De Wispelaere, L.; Hemp, A. Water-isotope ecohydrology of Mount Kilimanjaro. *Ecohydrology* **2020**, *13*, e2171. [[CrossRef](#)]
- Zhang, S.; Xiong, K.; Qin, Y.; Min, X.; Xiao, J. Evolution and determinants of ecosystem services: Insights from South China karst. *Ecol. Indic.* **2021**, *133*, 108437. [[CrossRef](#)]
- Tie, Q.; Hu, H.C.; Tian, F.Q. Environmental and physiological controls on sap flow in a subhumid mountainous catchment in North China. *Agric. For. Meteorol.* **2017**, *240–241*, 46–57. [[CrossRef](#)]
- Tang, Y.K.; Wen, X.F.; Sun, X.M. The limiting effect of deep soil water on evapotranspiration of a subtropical coniferous plantation subjected to seasonal drought. *Adv. Atmos. Sci.* **2014**, *31*, 385–395. [[CrossRef](#)]
- Fu, T.; Chen, H.; Wang, K. Structure and water storage capacity of a small karst aquifer based on stream discharge in South China. *J. Hydrol.* **2016**, *534*, 50–62. [[CrossRef](#)]
- Song, L.; Yang, B.; Liu, L.L.; Mo, Y.X.; Liu, W.J.; Meng, X.J.; Zhang, Y.J. Spatial-temporal differentiations in water use of coexisting trees from a subtropical evergreen broadleaved forest in Southwest China. *Agric. For. Meteorol.* **2022**, *316*, 108862. [[CrossRef](#)]
- Wang, X.; Liu, Z.; Xiong, K.; He, Q.; Li, Y.; Li, K. Characteristics and controlling factors of soil dissolved organic matter in the rainy season after vegetation restoration in a karst drainage area, South China. *Catena* **2022**, *217*, 106483. [[CrossRef](#)]
- Brinkmann, N.; Seeger, S.; Weiler, M. Employing stable isotopes to determine the residence times of soil water and the temporal origin of water taken up by *Fagus sylvatica* and *Picea abies* in a temperate forest. *New. Phytol.* **2018**, *219*, 1300–1313. [[CrossRef](#)] [[PubMed](#)]
- Rowland, L.; da Costa, A.C.; Galbraith, D.R.; Oliveira, R.S.; Binks, O.J. Death from drought in tropical forests is triggered by hydraulics not carbon starvation. *Nature* **2015**, *528*, 119–122. [[CrossRef](#)]
- Xiao, J.; Xiong, K. A review of agroforestry ecosystem services and its enlightenment on the ecosystem improvement of rocky desertification control. *Sci. Total Environ.* **2022**, *856*, 158538. [[CrossRef](#)]

17. Nie, Y.P.; Chen, H.S.; Wang, K.L.; Tan, W.; Deng, P.Y.; Yang, J. Seasonal water use patterns of woody species growing on the continuous dolostone outcrops and nearby thin soils in subtropical China. *Plant Soil*. **2011**, *341*, 399–412. [[CrossRef](#)]
18. Tu, Z.; Chen, S.; Chen, Z.; Ruan, D.; Zhang, W.; Han, Y.; Han, L.; Wang, K.; Huang, Y.; Chen, J. Hydrological Properties of Soil and Litter Layers of Four Forest Types Restored in the Gully Erosion Area of Latosol in South China. *Forests* **2023**, *14*, 360. [[CrossRef](#)]
19. Tang, Y.K.; Wu, X.; Chen, Y.M.; Wen, J.; Xie, Y.; Lu, S. Water use strategies for two dominant tree species in pure and mixed plantations of the semiarid Chinese Loess Plateau. *Ecohydrology* **2018**, *11*, e1943. [[CrossRef](#)]
20. Seneviratne, S.I.; Corti, T.; Davin, E.L. Investigating soil moisture–climate interactions in a changing climate: A review. *Earth Sci. Rev.* **2010**, *99*, 125–161. [[CrossRef](#)]
21. Xu, Q.; Xiong, K.; Chi, Y. Effects of intercropping on fractal dimension and physicochemical properties of soil in karst areas. *Forests* **2021**, *12*, 1422. [[CrossRef](#)]
22. Rothfuss, Y.; Javaux, M. Reviews and syntheses: Isotopic approaches to quantify root water uptake: A review and comparison of methods. *Biogeosciences* **2017**, *14*, 2199–2224. [[CrossRef](#)]
23. Wu, H.; Li, X.Y.; Jiang, Z.; Chen, H. Contrasting water use pattern of introduced and native plants in an alpine desert ecosystem, Northeast Qinghai–Tibet Plateau, China. *Sci. Total Environ.* **2016**, *542*, 182–191. [[CrossRef](#)] [[PubMed](#)]
24. Herberich, M.M.; Gayler, S.; Anand, M.; Tielbörger, K. Hydrological niche segregation of plant functional traits in an individual-based model. *Ecol. Model.* **2017**, *356*, 14–24. [[CrossRef](#)]
25. Liu, W.; Chen, H.; Zou, Q.; Nie, Y. Divergent root water uptake depth and coordinated hydraulic traits among typical karst plantations of subtropical China: Implication for plant water adaptation under precipitation changes. *Agric. Water Manag.* **2021**, *249*, 106798. [[CrossRef](#)]
26. Asbjornsen, H.; Shepherd, G.; Helmers, M. Seasonal patterns in depth of water uptake under contrasting annual and perennial systems in the Corn Belt Region of the Midwestern US. *Plant Soil* **2008**, *308*, 69–92. [[CrossRef](#)]
27. Fu, A.; Chen, Y.; Li, W. Water use strategies of the desert riparian forest plant community in the lower reaches of Heihe River Basin, China. *Sci. China Earth Sci.* **2014**, *57*, 1293–1305. [[CrossRef](#)]
28. Yang, B.; Wen, X.F.; Sun, X.M. Seasonal variations in depth of water uptake for a subtropical coniferous plantation subjected to drought in an East Asian monsoon region. *Agric. For. Meteorol.* **2015**, *201*, 218–228. [[CrossRef](#)]
29. Li, Y.; Liu, Z.; Liu, G. Dynamic Variations in Soil Moisture in an Epikarst Fissure in the Karst Rocky Desertification Area. *J. Hydrol.* **2020**, *591*, 1–12. [[CrossRef](#)]
30. Querejeta, J.I.; Estrada-Medina, H.; Allen, M.F.; Jimenez-Osornio, J. Water source partitioning among trees growing on shallow karst soils in a seasonally dry tropical climate. *Oecologia* **2007**, *152*, 26–36. [[CrossRef](#)]
31. Wen, X.; Lee, X.; Sun, X.; Wang, J.; Hu, Z.; Li, S.; Yu, G. Dew water isotopic ratios and their relationships to ecosystem water pools and fluxes in a cropland and a grassland in China. *Oecologia* **2012**, *168*, 549–561. [[CrossRef](#)]
32. Schultz, N.M.; Griffis, T.J.; Lee, X.; Baker, J.M. Identification and correction of spectral contamination in 2H/1H and 18O/16O measured in leaf, stem, and soil water. *Rapid Commun. Mass Spectrom.* **2011**, *25*, 3360–3368. [[CrossRef](#)]
33. Stock, B.; Semmens, B. *MixSIAR GUI User Manual v3. 1.*; Scripps Institution of Oceanography, UC San Diego: San Diego, CA, USA, 2016.
34. Fan, J.; Wang, Q.; Jones, S.B. Soil water depletion and recharge under different land cover in China’s Loess Plateau. *Ecohydrology* **2016**, *9*, 396–406. [[CrossRef](#)]
35. Craig, H. Isotopic variations in meteoric waters. *Science* **1961**, *133*, 1702–1703. [[CrossRef](#)]
36. Renée Brooks, J.; Barnard, H.R.; Coulombe, R.; McDonnell, J.J. Ecohydrologic separation of water between trees and streams in a Mediterranean climate. *Nat. Geosci.* **2010**, *3*, 100–104. [[CrossRef](#)]
37. Geris, J.; Tetzlaff, D.; McDonnell, J.J. Spatial and temporal patterns of soil water storage and vegetation water use in humid northern catchments. *Sci. Total. Environ.* **2017**, *595*, 486–493. [[CrossRef](#)]
38. Han, C.; Chen, N.; Zhang, C.; Liu, Y. Sap flow and responses to meteorological about the *Larix principis-rupprechtii* plantation in Gansu Xinlong mountain, northwestern China. *For. Ecol. Manag.* **2019**, *451*, 117519. [[CrossRef](#)]
39. Dong, Z.; Li, S.; Zhao, Y.; Lei, J.; Wang, Y.; Li, C. Stable oxygen-hydrogen isotopes reveal water use strategies of *Tamarix taklamakanensis* in the Taklimakan Desert, China. *J. Arid Land* **2020**, *12*, 115–129. [[CrossRef](#)]
40. Jiang, Z.C.; Lian, Y.Q.; Qin, X.Q. Rocky desertification in Southwest China: impacts, causes, and restoration. *Earth-Sci. Rev.* **2014**, *132*, 1–12. [[CrossRef](#)]
41. Xiang, W.; Si, B.C.; Biswas, A.; Li, Z. Quantifying dual recharge mechanisms in deep unsaturated zone of Chinese Loess Plateau using stable isotopes. *Geoderma* **2019**, *337*, 773–781. [[CrossRef](#)]
42. Demand, D.; Blume, T.; Weiler, M. Spatio-temporal relevance and controls of preferential flow at the landscape scale. *Hydrol. Earth Syst. Sci.* **2019**, *23*, 4869–4889. [[CrossRef](#)]
43. Gazis, C.; Feng, X. A stable isotope study of soil water: Evidence for mixing and preferential flow paths. *Geoderma* **2004**, *119*, 97–111. [[CrossRef](#)]
44. Chen, F.; Huang, C.; Lao, Q.; Zhang, S.; Chen, C.; Zhou, X.; Zhu, Q. Typhoon control of precipitation dual isotopes in southern China and its palaeoenvironmental implications. *J. Geophys. Res. Atmos.* **2021**, *126*, e2020JD034336. [[CrossRef](#)]
45. Tian, L.; Yao, T.; Sun, W.; Stievenard, M.; Jouzel, J. Relationship between δD and $\delta^{18}O$ in precipitation on north and south of the Tibetan Plateau and moisture recycling. *Sci. China Ser. D Earth Sci.* **2001**, *44*, 789–796. [[CrossRef](#)]

46. Wu, X.; Pan, M.; Zhu, X.; Yin, J.; Wang, Z.; Zhang, M.; Cao, J. Effect of the El Niño–Southern Oscillation on hydrogen and oxygen isotope ratios of precipitation in Guilin, SW China. *Isot. Environ. Health Stud.* **2021**, *57*, 67–81. [[CrossRef](#)] [[PubMed](#)]
47. Wang, J.; Fu, B.J.; Lu, N.; Zhang, L. Seasonal variation in water uptake patterns of three plant species based on stable isotopes in the semi-arid Loess Plateau. *Sci. Total Environ.* **2017**, *609*, 27–37. [[CrossRef](#)]
48. Gao, X.D.; Zhao, X.N.; Wu, P.T.; Brocca, L.; Zhang, B.Q. Effects of large gullies on catchment-scale soil moisture spatial behaviors: A case study on the Loess Plateau of China. *Geoderma* **2016**, *261*, 1–10. [[CrossRef](#)]
49. Flanagan, L.B.; Orchard, T.E.; Tremel, T.N. Using stable isotopes to quantify water sources for trees and shrubs in a riparian cottonwood ecosystem in flood and drought years. *Hydrol. Process.* **2019**, *33*, 3070–3083. [[CrossRef](#)]
50. Leite, P.A.; Wilcox, B.P.; McInnes, K.J. Woody plant encroachment enhances soil infiltrability of a semiarid karst savanna. *Environ. Res. Commun.* **2020**, *2*, 115005. [[CrossRef](#)]
51. Hoekstra, N.J.; Finn, J.A.; Hofer, D. The effect of drought and interspecific interactions on depth of water uptake in deep- and shallow-rooting grassland species as determined by $\delta^{18}\text{O}$ natural abundance. *Biogeosciences* **2014**, *11*, 4493–4506. [[CrossRef](#)]
52. Karakis, S.; Gulbranson, E.; Cameron, B. Insight into the source of grapevine water acquisition during key phenological stages using stable isotope analysis. *Aust. J. Grape Wine Res.* **2018**, *24*, 252–259. [[CrossRef](#)]
53. Barbeta, A.; Mejía-Chang, M.; Ogaya, R.; Voltas, J.; Dawson, T.; Peñuelas, J. The combined effects of a long-term experimental drought and an extreme drought on the use of plant-water sources in a Mediterranean forest. *Glob. Change Biol.* **2015**, *21*, 1213–1225. [[CrossRef](#)] [[PubMed](#)]
54. Feng, X.; Fu, B.; Piao, S.; Wang, S.; Ciais, P.; Zeng, Z.; Wu, B. Revegetation in China’s Loess Plateau is approaching sustainable water resource limits. *Nat. Clim. Change* **2016**, *6*, 1019–1022. [[CrossRef](#)]
55. Luo, Y.; Gong, Y. α Diversity of Desert Shrub Communities and Its Relationship with Climatic Factors in Xinjiang. *Forests* **2023**, *14*, 178. [[CrossRef](#)]
56. Apostolakis, A.; Schöning, I.; Michalzik, B.; Ammer, C.; Schall, P.; Hänsel, F.; Nauss, T.; Trumbore, S.; Schruppf, M. Forest Structure and Fine Root Biomass Influence Soil CO₂ Efflux in Temperate Forests under Drought. *Forests* **2023**, *14*, 411. [[CrossRef](#)]
57. Jiang, Y.; Huang, A.; Wu, H.; Zhang, X. GIS-based research on climate suitable region of Loquat in Lishui, Zhejiang province of China. *Environ. Res. Commun.* **2022**, *4*, 015006. [[CrossRef](#)]
58. Zhang, Y.; Yao, Q.; Li, J.; Wang, Y.; Liu, X.; Hu, Y.; Chen, J. Contributions of an arbuscular mycorrhizal fungus to growth and physiology of loquat (*Eriobotrya japonica*) plants subjected to drought stress. *Mycol. Prog.* **2015**, *14*, 1–11. [[CrossRef](#)]
59. Mao, Q.; He, B.; Ma, M.; Wang, L.; Koike, T.; Agathokleous, E. Effects of biochar on Karst lime soil nutrients, soil microbial communities, and physiology of Sichuan pepper plants. *Ann. Appl. Biol.* **2022**, *181*, 357–366. [[CrossRef](#)]
60. Zhang, F.; Jia, W.; Zhu, G.; Zhang, Z.; Shi, Y.; Yang, L.; Zhang, M. Using stable isotopes to investigate differences of plant water sources in subalpine habitats. *Hydrol. Process.* **2022**, *36*, e14518. [[CrossRef](#)]
61. Li, T.; Liu, Y.; Cai, Q.; Duan, X.; Li, P.; Ren, M.; Ye, Y. Water Stress-Induced Divergence Growth of *Picea schrenkiana* in the Western Tianshan and Its Forcing Mechanisms. *Forests* **2023**, *14*, 354. [[CrossRef](#)]
62. Taufik, M.; Torfs, P.J.; Uijlenhoet, R.; Jones, P.D.; Murdiyarso, D.; Van Lanen, H.A. Amplification of wildfire area burnt by hydrological drought in the humid tropics. *Nat. Clim. Change* **2017**, *7*, 428. [[CrossRef](#)]
63. Sterck, F.; Markesteijn, L.; Schieving, F.; Poorter, L. Functional traits determine trade-offs and niches in a tropical forest community. *Proc. Natl. Acad. Sci. USA* **2011**, *108*, 20627–20632. [[CrossRef](#)] [[PubMed](#)]
64. Jiang, S.; Xiong, K.; Xiao, J. Structure and Stability of Agroforestry Ecosystems: Insights into the Improvement of Service Supply Capacity of Agroforestry Ecosystems under the Karst Rocky Desertification Control. *Forests* **2022**, *13*, 878. [[CrossRef](#)]
65. Ivanov, V.Y.; Hutyra, L.R.; Wofsy, S.C.; Munger, J.W.; Saleska, S.R.; De Oliveira, R.C.; De Camargo, P.B. Root niche separation can explain avoidance of seasonal drought stress and vulnerability of overstorey trees to extended drought in a mature Amazonian forest. *Water Resour. Res.* **2012**, *48*, 1–21. [[CrossRef](#)]
66. McDowell, N.G.; Allen, C.D. Darcy’s law predicts widespread forest mortality under climate warming. *Nat. Clim. Change* **2015**, *5*, 669–672. [[CrossRef](#)]
67. Karger, D.N.; Kessler, M.; Lehnert, M.; Jetz, W. Limited protection and ongoing loss of tropical cloud forest biodiversity and ecosystems worldwide. *Nat. Ecol. Evol.* **2021**, *5*, 854–862. [[CrossRef](#)]
68. Silvertown, J.; Araya, Y.; Gowing, D. Hydrological niches in terrestrial plant communities: A review. *J. Ecol.* **2015**, *103*, 93–108. [[CrossRef](#)]
69. Restrepo-Coupe, N.; Levine, N.M.; Christoffersen, B.O.; Albert, L.P.; Wu, J.; Costa, M.H.; Saleska, S.R. Do dynamic global vegetation models capture the seasonality of carbon fluxes in the Amazon basin? A data-model intercomparison. *Glob. Change Biol.* **2016**, *23*, 1–18. [[CrossRef](#)]
70. Meinzer, F.C.; Johnson, D.M.; Lachenbruch, B.; McCulloh, K.A.; Woodruff, D.R. Xylem hydraulic safety margins in woody plants: Coordination of stomatal control of xylem tension with hydraulic capacitance. *Funct. Ecol.* **2009**, *23*, 922–930. [[CrossRef](#)]
71. Deng, X.; Xiong, K.; Yu, Y.; Zhang, S.; Kong, L.; Zhang, Y. A Review of Ecosystem Service Trade-Offs/Synergies: Enlightenment for the Optimization of Forest Ecosystem Functions in Karst Desertification Control. *Forests* **2023**, *14*, 88. [[CrossRef](#)]
72. Guo, W.; Liu, H.; Wu, X. Vegetation greening despite weakening coupling between vegetation growth and temperature over the boreal region. *J. Geophys. Res. Biogeosci.* **2018**, *123*, 2376–2387. [[CrossRef](#)]
73. Feng, H.; Zou, B. A greening world enhances the surface-air temperature difference. *Sci. Total Environ.* **2019**, *658*, 385–394. [[CrossRef](#)]

74. Yang, J.; Chen, H.; Nie, Y.; Wang, K. Dynamic variations in profile soil water on karst hillslopes in South China. *Catena* **2019**, *172*, 655–663. [[CrossRef](#)]
75. Huo, G.P.; Zhao, X.N.; Gao, X.D.; Wang, S.F.; Pan, Y.H. Seasonal water use patterns of rainfed jujube trees in stands of different ages under semiarid plantations in China. *Agric. Ecosyst. Environ.* **2018**, *265*, 392–401. [[CrossRef](#)]
76. Ellsworth, P.Z.; Sternberg, L.S. Seasonal water use by deciduous and evergreen woody species in a scrub community is based on water availability and root distribution. *Ecohydrology* **2015**, *8*, 538–551. [[CrossRef](#)]

Disclaimer/Publisher’s Note: The statements, opinions and data contained in all publications are solely those of the individual author(s) and contributor(s) and not of MDPI and/or the editor(s). MDPI and/or the editor(s) disclaim responsibility for any injury to people or property resulting from any ideas, methods, instructions or products referred to in the content.